

## DISCOVERY OF A SYMMETRICAL HIGHLY COLLIMATED BIPOLAR JET IN HEN 2-90<sup>1</sup>

RAGHVENDRA SAHAI<sup>2</sup> AND LARS-ÅKE NYMAN<sup>3</sup>

Received 2000 March 31; accepted 2000 May 22; published 2000 July 28

### ABSTRACT

Using the *Hubble Space Telescope*, we have obtained H $\alpha$  imaging of the object Hen 2-90, which has long been classified as a planetary nebula (PN). We find that the morphology of Hen 2-90 does not look like that of any known PN, but resembles that of a classical young stellar object (YSO)—a bipolar nebula bisected by a flaring disklike structure and a highly collimated bipolar jet perpendicular to the disk. The linear jet shows at least six pairs of emission knots located symmetrically on either side of the nebular center. Taking a kinematic distance of 2.5 kpc, we find that the gas density in the knots decreases steadily from about  $10^4 \text{ cm}^{-3}$  in the knots closest to the center to  $1.1 \times 10^3 \text{ cm}^{-3}$  in the more distant knots, and their masses lie in the range of  $(0.7\text{--}3.6) \times 10^{-6} M_{\odot}$ . The jet opening angle is about  $4^\circ$ , from which we estimate its speed to be  $\sim 150 \text{ km s}^{-1}$ . Hen 2-90's near- and mid-infrared fluxes imply the presence of a massive dusty nebula containing “warm” (183 K) and “hot” (513 K) dust in components with masses  $5 \times 10^{-3}$  and  $2.4 \times 10^{-5} M_{\odot}$ , respectively (assuming a gas-to-dust ratio of 100); the source luminosity is  $5280 L_{\odot}$ . Millimeter-wave line observations show no molecular gas directly associated with the source and the absence of star-forming activity, indicating that Hen 2-90 is probably not a YSO. The most likely hypothesis for explaining Hen 2-90 requires a binary with a cool giant and a compact companion with an accretion disk.

*Subject headings:* circumstellar matter — planetary nebulae: general — stars: AGB and post-AGB — stars: mass loss

### 1. INTRODUCTION

We have imaged Hen 2-90, an object discovered by Henize (1967) and listed as PK 305+1°1 in the Perek & Kohoutek (1967) Catalog of Galactic Planetary Nebulae (CGPN), with the *Hubble Space Telescope* (HST) as part of an H $\alpha$  imaging survey of young planetary nebulae (PNe; Sahai & Trauger 1998). We find that Hen 2-90 has the disk/jet morphology of a low-mass young stellar object (YSO), never seen before in PNe. In this Letter, we present our images of this apparently unique object and discuss its characteristics in the context of various evolutionary models; detailed analysis and follow-up multiwavelength observations (in progress) are deferred to a second paper (R. Sahai et al. 2000, in preparation).

### 2. OBSERVATIONS AND RESULTS

Six H $\alpha$  (with filter F656N) exposures of Hen 2-90 ( $2 \times 20$ ,  $2 \times 140$ ,  $2 \times 400$  s) were obtained in the Planetary Camera (800  $\times$  800 pixels; plate scale =  $0''.0456 \text{ pixel}^{-1}$ ) of the Wide Field Planetary Camera 2 (WFPC2) as part of our SNAPshot program (number 8345). Each image of an equal-exposure pair was shifted with respect to the other during the observations. A geometric distortion correction was applied to the pipeline-calibrated images, which were then registered to subpixel accuracy, followed by cosmic-ray removal and correction of saturated pixels. Millimeter-wave spectra were obtained using the 15 m Swedish-ESO-Submillimeter Telescope (SEST), in La Silla, Chile, using SIS receivers with single sideband (SSB)

system temperatures, respectively, of about 300 and 150–300 K in the 1.3 and 3 mm bands, and an Acousto-Optical Spectrometer (bandwidth 80 MHz, channel separation 43 kHz). The data were taken in a position-switched mode with an off position 2.5 away in declination. All intensities are given in main-beam brightness temperatures ( $T_{\text{mb}}$ ).

#### 2.1. Optical Morphology

The F656N image of Hen 2-90 (Figs. 1 and 2) shows a highly collimated, linear, bipolar jet emerging from a central bipolar nebula (“core”), bisected by a flaring, dark, disk structure orthogonal to the jet. The jet shows at least six pairs of emission knots (labeled  $a$ – $f$  and  $a'$ – $f'$ ) located symmetrically on either side of the nebular center (J2000 coordinates:  $\alpha = 13^{\text{h}}09^{\text{m}}36^{\text{s}}.39$ ,  $\delta = -61^\circ19'36''.3$ ), defined as the intersection of the jet axis and the disk midplane (Fig. 3). *No central star is visible* (Fig. 2), indicating that the dense disk is seen almost edge-on. The northwest lobe is brighter than the southeast one by a factor  $\approx 7$ , implying that the northwest face of the disk, and by inference the northwest side of the jet, is tilted toward us. The tilt angle is probably small ( $<10^\circ$ – $15^\circ$ , by comparison with, e.g., HH 30; Burrows et al. 1996). New ground-based imaging of Hen 2-90 (R. Sahai et al. 2000, in preparation) shows that the jet extends to  $\approx 30''$  on either side. The core is surrounded by a round halo; a significant fraction ( $\sim 20\%$ – $50\%$ , depending on location) of the halo light is due to the wings of the point-spread function of the northwest lobe. The core is very bright compared to the knots and halo, e.g., its flux (in a  $0''.46 \times 0''.46$  aperture) is about 1000 times greater than that of knots  $a$  and  $a'$  (in a  $0''.34 \times 0''.34$  aperture) and about 59% of the total nebular flux ( $3.2 \times 10^{-11} \text{ ergs s}^{-1} \text{ cm}^{-2}$ ).

The near-kinematic distance to Hen 2-90, based on its optical radial velocity of  $-31 \text{ km s}^{-1}$   $V_{\text{LSR}}$ , is 2.8 kpc, assuming Galactic parameters  $R_0 = 8.5 \text{ kpc}$  and  $\Theta_0 = 220 \text{ km s}^{-1}$  (e.g., Maciel & Dutra 1992); the far-kinematic distance (6.9 kpc) is unlikely in view of the modest extinction,  $E(B-V) = 1.3$ , de-

<sup>1</sup> Based on observations with the NASA/ESA *Hubble Space Telescope*, obtained at the Space Telescope Science Institute, which is operated by the Association of Universities for Research in Astronomy, Inc., under NASA contract NAS5-26555.

<sup>2</sup> Jet Propulsion Laboratory, MS 183-900, California Institute of Technology, Pasadena, CA 91109.

<sup>3</sup> European Southern Observatory, Santiago 19, Chile; and Onsala Space Observatory, S-43992 Onsala, Sweden.

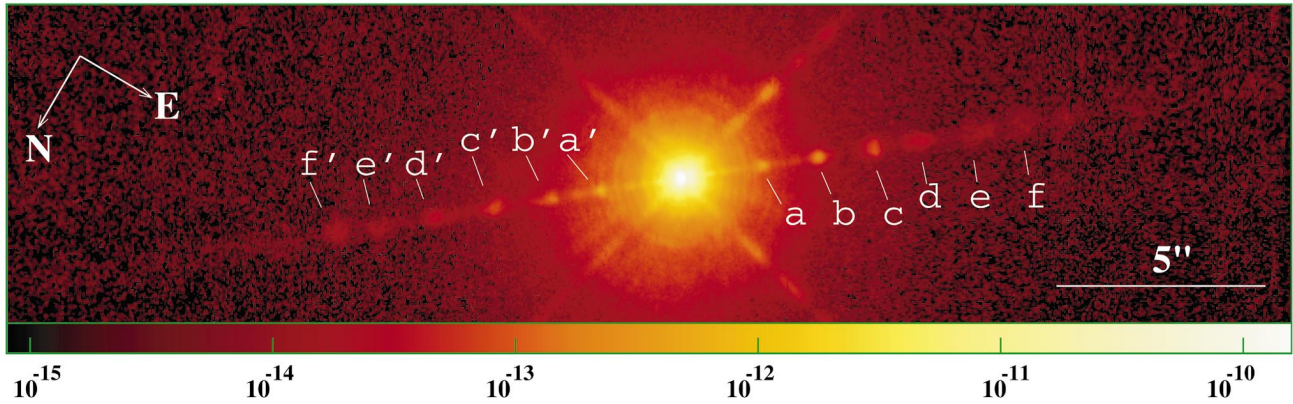


FIG. 1.— $H\alpha$  (F656N) image of Hen 2-90 taken with the Planetary Camera (resolution  $0''.0456 \text{ pixel}^{-1}$ ) of WPC2/HST (logarithmic stretch). The very bright central source results in strong diffraction spikes at  $\pm 45^\circ$  in the image due to support structures in the telescope. No image artifacts are expected at the orientation of the observed jet. The maximum and minimum surface brightnesses on the scale bar shown are  $1.58 \times 10^{-10}$  and  $7.90 \times 10^{-16} \text{ ergs s}^{-1} \text{ cm}^{-2} \text{ arcsec}^{-2}$ .

rived toward Hen 2-90 (Costa, de Freitas Pacheco, & Maciel 1993, hereafter CFPM93). CFPM93 derive a distance of 1.5 kpc based on a radius of  $6''$  using the Shlovsky method, but the peculiar morphology and size of Hen 2-90 makes this estimate questionable. However, if Hen 2-90 is photoionized by stellar UV, then  $T_{\text{eff}} > 30,000 \text{ K}$  (the nebular spectrum indicates  $\sim 50,000 \text{ K}$ ; see § 3); if it is unevolved, its spectral type must be earlier than B0, implying  $L > 2 \times 10^4 L_\odot$  and  $D > 4.9 \text{ kpc}$  from its bolometric flux (see § 2.2). If the central star is evolved, it is a white dwarf; then if it ejected the dense, compact, ionized nebula around it, Hen 2-90 is a young PN and  $L \gtrsim 10^3 L_\odot$  (e.g., Wood & Faulkner 1991), implying  $D \gtrsim 1.1 \text{ kpc}$ . We adopt  $D = 2.5 \text{ kpc}$  for Hen 2-90 and provide the distance dependencies of derived physical parameters.

The jet can be traced to within  $0''.4$  (1000 AU) of the center (Fig. 4), where its width is about  $0''.06$  (150 AU). The jet

morphology indicates a jet opening angle roughly constant with distance from center. We find that the *apparent* jet opening angle at any knot,  $\theta_p$  (FWHM of the Gaussian fit to the intensity), decreases from  $5.5^\circ$  at knots  $a$  and  $a'$  to  $3.9^\circ$  at knots  $b, c, b',$  and  $c'$  and  $3.2^\circ$  at knots  $d, e, d',$  and  $e'$  with uncertainties of  $\lesssim 10\%$ . This marginal radial decrease in the jet opening angle may be due to a decrease in the temperature of the knots due to cooling by adiabatic expansion and/or mild recollimation of the jet. The centers of knots  $a-e$  and  $a'-e'$  lie along a straight line with P.A. =  $129.3^\circ \pm 0.25^\circ$ .

We now make rough estimates of the physical properties of the jet and its knots from their excess (over the surrounding diffuse emission) peak  $H\alpha$  surface brightness  $I(H\alpha)$ , assuming case B recombination, and an electron temperature of  $10^4 \text{ K}$ .  $I(H\alpha)$  varies from about  $3.5 \times 10^{-13}$  to  $7.5 \times 10^{-15} \text{ ergs s}^{-1} \text{ cm}^{-2} \text{ arcsec}^{-2}$  in going from knots  $a$  and  $a'$  to knots  $e$  and  $e'$ . Approximating each knot as a constant-density sphere of diameter equal to its FWHM size, we find that the gas density ( $\propto D^{-0.5}$ ) decreases steadily from about  $9.7 \times 10^3 \text{ cm}^{-3}$  in knots  $a$  and  $a'$  to  $1.2 \times 10^3 \text{ cm}^{-3}$  in knots  $e$  and  $e'$ . In comparison, a similar estimate for the bright lobe of the core gives a density of  $2.8 \times 10^5 \text{ cm}^{-3}$  (ignoring complications due to disk scattering of photons emitted near the star), consistent with

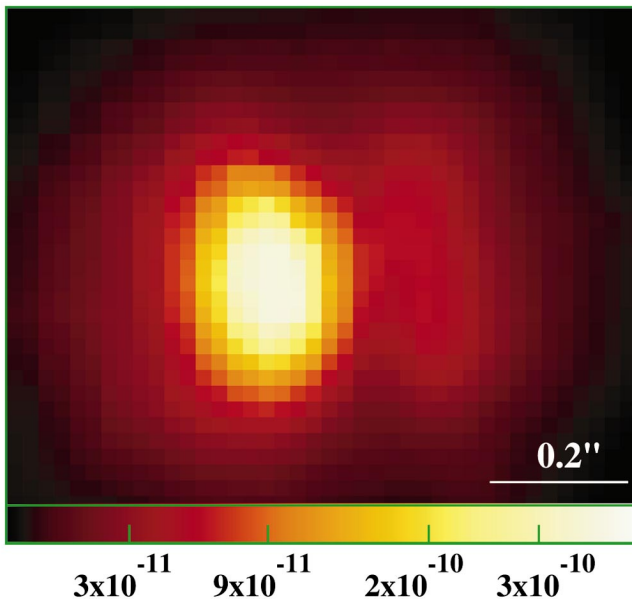


FIG. 2.—Central region of the image in Fig. 1, showing a bipolar nebula with a roughly edge-on disk (square-root stretch). The maximum and minimum surface brightnesses on the scale bar shown are  $4.05 \times 10^{-10}$  and  $3.64 \times 10^{-12} \text{ ergs s}^{-1} \text{ cm}^{-2} \text{ arcsec}^{-2}$ .

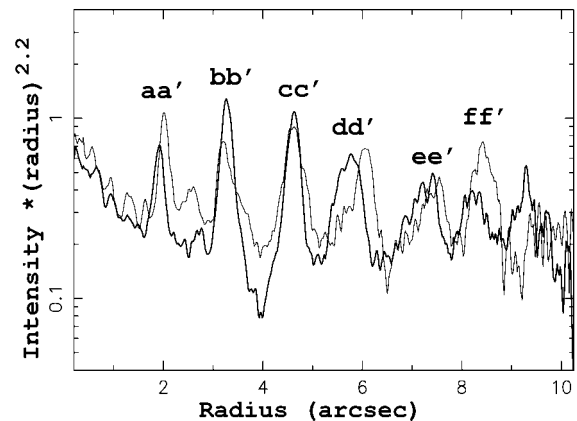


FIG. 3.—Relative intensity of the jet as a function of radius  $r$  showing the radial offsets of the knots from the center (thick curve: southeast jet, thin curve: northwest jet). The steeply falling intensity has been scaled by  $r^{2.2}$ .

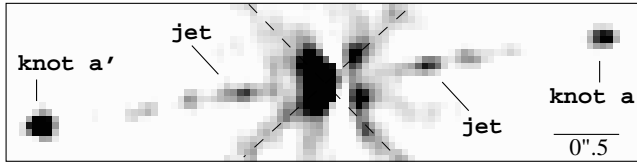


FIG. 4.—Image of the central region processed to enhance sharp features. The processed image  $Im_p = [Im_o/(Im_o + 0.09Im_s)]^4$ , where  $Im_o$  is the original image (in Fig. 1) and  $Im_s$  is obtained by smoothing  $Im_o$ . The jet can be traced to within  $0''.4$  of the center of the nebula. Dashed lines mark the diffraction spikes due to support structures in the telescope.

CFMP93's value ( $\sim 10^5 \text{ cm}^{-3}$ ). The knot masses ( $\propto D^{2.5}$ ) lie in the range  $(0.75\text{--}3.6) \times 10^{-6} M_\odot$ ; knots  $c$  and  $c'$  have the largest mass. Since the ionization fraction in the knots may be less than unity, the above masses are lower limits. The interknot jet region is fainter than the knots by factors of 3–9. Assuming a constant jet outflow velocity ( $V_j$ ) and free transverse expansion,  $V_j = c_{s,j}/[\theta_p \cos(i)]$ , where  $c_{s,j}$  is the sound speed in the knots, and  $i$  is the (small) tilt angle. We find that  $V_j \sim 150 \text{ km s}^{-1}$ , setting  $\theta_p = 4^\circ$  and assuming  $c_{s,j} = 10 \text{ km s}^{-1}$  for ionized gas at  $10^4 \text{ K}$ . However, since the knots appear non-spherical, most likely due to dynamic interactions that can induce turbulent motions several times larger than the sound speed  $c_{s,j}$ , the jet velocity derived above is probably an uncertain lower limit, and the ages of the jet material (derived below) are upper limits. Thus the jet is relatively young; knots  $a$ – $f$  and  $a'$ – $f'$  were ejected over the past 160–700 yr, at roughly regular intervals of 100–120 yr; the youngest visible jet material was ejected about 30 yr ago (the ages scale as  $D$  and do not depend on  $i$ ). The peak mass-loss rates in the knots are about  $(1\text{--}2) \times 10^{-8} (D/2.5 \text{ kpc})^{1.5} M_\odot \text{ yr}^{-1}$ .

## 2.2. Molecular Gas, Dust, and Luminosity

We detected and mapped CO emission toward Hen 2-90. The  $J = 1\text{--}0$  and  $2\text{--}1$  line profiles observed toward the Hen 2-90 position are centered at  $-29 \text{ km s}^{-1} V_{\text{LSR}}$ , roughly Gaussian and narrow (FWHM  $\sim 3 \text{ km s}^{-1}$ ). Our map (with a  $45''$  beam) of the  $1\text{--}0$  line shows very extended emission (Fig. 5) with a complex spatio-kinematic structure; the line profiles become wider in some positions, perhaps due to blending of several components at different velocities. There is also weaker CO emission in the velocity range  $-50$  to  $-45 \text{ km s}^{-1} V_{\text{LSR}}$  toward the east and south, coming from other line-of-sight molecular clouds. The peak CO and optical radial velocities of Hen 2-90 are in good agreement, but since the CO emission is very extended and the narrow, Gaussian-shaped lines do not resemble the broad circumstellar lines typical of PNe, we believe that it arises in interstellar gas which is near but not directly related to Hen 2-90. The CO  $J = 2\text{--}1$  to  $1\text{--}0$  line intensity ratio ( $<1$ ) indicates that both lines are optically thick and have a relatively low excitation temperature ( $\approx 8 \text{ K}$ ). We did not detect the CS ( $2\text{--}1$ ) ( $<30 \text{ mK}$ ,  $1 \sigma$ ) or CS ( $5\text{--}4$ ) ( $<120 \text{ mK}$ ,  $1 \sigma$ ) lines; this result and the low gas temperature indicate the absence of a dense, star-forming core toward Hen 2-90.

*IRAS* broadband photometric measurements and LRS spectra and the (archival) *Infrared Space Observatory* (*ISO*) SWS/LWS spectra of Hen 2-90 clearly show the presence of a cool dusty envelope around the central star. We have fitted Hen 2-90's color-corrected *IRAS* fluxes (56.1, 69.2, 15.6, and  $<46 \text{ Jy}$  at 12, 25, 60, and  $100 \mu\text{m}$ ), the (relatively uncertain) *ISO* LWS

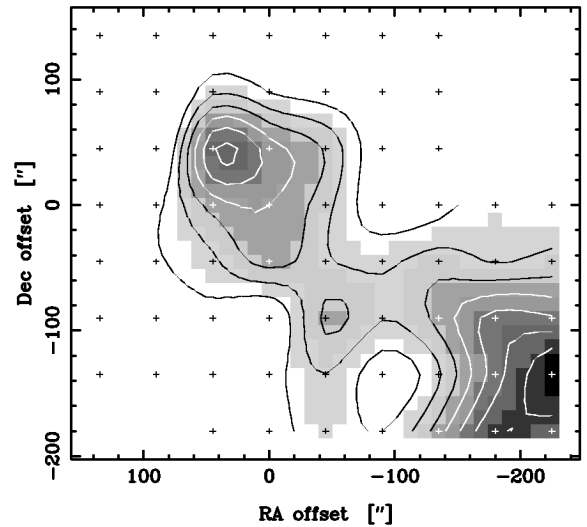


FIG. 5.—Map of the CO  $J = 1\text{--}0$  emission intensity integrated between  $-35$  and  $-26 \text{ km s}^{-1} V_{\text{LSR}}$  toward Hen 2-90. The contours are 20%, 30%, ... of the peak intensity of  $12.5 \text{ K km s}^{-1}$ .

$100 \mu\text{m}$  flux of  $10 \text{ Jy}$  and the  $L$ - and  $K$ -band fluxes ( $4.8$  and  $0.46 \text{ Jy}$ ; Acker et al. 1992) using a multicomponent model (Sahai et al. 1991). Assuming a power-law ( $\lambda^{-p}$ , with  $p = 1$ ) dust emissivity with a value of  $150 \text{ cm}^2 \text{ g}^{-1}$  at  $60 \mu\text{m}$  (Jura 1986) and a gas-to-dust ratio of 100, our best-fit model requires “warm” ( $183 \text{ K}$ ) and “hot” ( $513 \text{ K}$ ) dust in components of masses  $5 \times 10^{-3}$  and  $2.4 \times 10^{-5} M_\odot$ , respectively (the masses scale as  $D^2$ ). Although most of the dust mass is in the warm component, the hot component emits roughly half of the total luminosity,  $L = 5280 (D/2.5 \text{ kpc})^2 L_\odot$ . The bolometric flux is  $2.7 \times 10^{-8} \text{ ergs s}^{-1} \text{ cm}^{-2}$ .

## 3. DISCUSSION: THE NATURE OF HEN 2-90

Although both direct and indirect evidence exists for the presence of collimated outflows and jets in PNe (e.g., Sahai & Trauger 1998; Harrington & Borkowski 2000), Hen 2-90's morphology does not resemble that of any known PN (all resolved PNe show shells and/or limb-brightened lobes). But, since at least one PN (IC 4593; Harrington & Borkowski) shows a well-collimated jet with a pair of knots around the center, it is possible that Hen 2-90 is a PN. Nevertheless, the strong morphological similarity between Hen 2-90 and low-mass YSOs (e.g., HH 30; Burrows et al. 1996) forces us to reexamine Hen 2-90's classification as a PN. Hen 2-90 is very unlikely to be a *low-mass* pre-main-sequence star because it is too luminous (§ 2.1). In the Acker et al. (1992) catalog of PNe which lists Hen 2-90, only 1143 out of a total 1820 objects classified at least once as PNe were retained; many were rejected as being *ultracompact H II regions* (UCHRs). However, UCHRs normally do not show [O III] ( $\lambda 5007$ ) emission (e.g., Kimeswenger 1998) but Hen 2-90 does, consistent with the  $51,000 \text{ K } T_{\text{eff}}$  determined for its central star (Kaler & Jacoby 1991; Preite-Martinez et al. 1991). Hen 2-90 lies roughly in between the adjacent regions occupied by PNe and OH/IR stars in the *IRAS* color-color diagram ( $F_{\lambda}[12]/F_{\lambda}[25]$  vs.  $F_{\lambda}[25]/F_{\lambda}[60]$ ; Pottasch et al. 1988), far removed from UCHRs, whose mid-IR spectra peak at much longer wavelengths ( $\lambda \gtrsim 100 \mu\text{m}$ ; e.g., Volk & Cohen 1990), indicative of significantly cooler dust. In the

emission-line diagnostic diagram (plot of the intensity ratios  $H\alpha/[N\ II]$  vs.  $H\alpha/[S\ II]$ ; e.g., Garcia-Lario et al. 1991), we find (using CFPM93's extinction-corrected line intensities) that Hen 2-90 is located in the vicinity of the PN region and well removed from UCHRs.

*Emission-line stars* have also been misclassified with PNe, since striking spectral similarities exist between stars showing the B[e] phenomenon (B-type stars with forbidden optical emission lines) and CGPN objects (Swings & Andrillat 1979). In their study of the B[e] star phenomenon, Lamers et al. (1998) classified Hen 2-90 as a "compact planetary nebula B[e] (cPNB[e]) star." We now further examine two other B[e] classes from Lamers et al. which contain luminous objects, often with evidence of collimated outflows. The first is the class of *H Ae B[e]* stars—pre-main-sequence stars with  $L \leq 3 \times 10^4 L_{\odot}$ . These stars in particular, and the general class of luminous [ $\log(L/L_{\odot}) \geq 3$ ] YSOs powering collimated outflows (which includes optically obscured objects like IRAS 18162–2048 [Martí, Rodríguez, & Reipurth 1993] and very luminous FU Ori stars like Z Cma [Poetzel, Mundt, & Ray 1989]), are associated with star-forming clouds and have cool *IRAS* colors like UCHRs. However, as our SEST data show, the molecular cloud observed toward Hen 2-90 is unlikely to be a star-forming region (§ 2.2), and its *IRAS* colors are significantly hotter.

The second class, *symbiotic B[e] stars*, are interacting binaries composed of a cool giant and a hot compact object (such as a white dwarf), often surrounded by a nebula. Some symbiotic stars show fast outflows (e.g., Corradi et al. 1999), and the collimated R Aqr jet shows several emission knots on either side of the central binary (e.g., Hollis et al. 1997; Kafatos et al. 1989). *Could Hen 2-90 be a symbiotic system like R Aqr?* The very low abundances of O, N, Ne, and Ar derived for Hen 2-90 by CFPM93 argue for the presence of an evolved star. Most physical mechanisms for astrophysical jets invoke accretion disks; such disks are expected to form in a symbiotic system through Roche lobe overflow and/or partial capture of the wind from the cool giant (Morris 1987). Although the disk seen in Hen 2-90's central bipolar nebula is too large for an accretion disk, it may represent the related "excretion" disk hypothesized by Morris. The hot (500 K) dust inferred in Hen 2-90 (§ 2.2) may then be associated with the inner regions of this disk. Possible signatures of a cool giant include (1) optical TiO absorption bands (unless it is heavily obscured), (2) strong near-infrared continuum, and (3) long-period ( $\sim 1$  yr) variations. TiO bands may be difficult to discern in the emission-line-dominated Hen 2-90 spectrum (and are not mentioned by CFPM93). However, unlike R Aqr and most cool giants, which show long-period variability, Hen 2-90 has a zero *IRAS* variability index, and in addition, there is good agreement between its 12–25  $\mu\text{m}$  fluxes from *IRAS* and the recent Midcourse Space

Experiment (MSX) Galactic plane survey (Egan et al. 1999), arguing for the lack of significant variations in Hen 2-90's mid-IR flux on a  $\sim 15$  yr timescale. Hen 2-90's radio continuum fluxes at 5, 8.9, and 14.5 GHz can be fitted with a power law ( $S_{\nu} \propto \nu^{\alpha}$ ) with  $\alpha = 1.55 \pm 0.29$ , but these data are insufficient for providing a strong diagnostic indication for the nature of the source (Purton et al. 1982). For comparison, we note that in symbiotic stars,  $\alpha \sim 0$ –1.2, with a most likely value near unity (Taylor & Seaquist 1984).

Hen 2-90 lies within the 99% position-error contour (of size  $0^{\circ}9 \times 0^{\circ}6$ ) of a  $\gamma$ -ray source (3EG J1308–6112, GRO J1308–61) with a flux of  $2.2 \times 10^{-7}$  photons  $\text{cm}^{-2} \text{s}^{-1}$  and a relatively steep spectral index of 3.1 (Hartman et al. 1999). The object 3EG J1308–6112 was detected only in period 1 with a total of 212 counts; upper limits for periods 2, 3, and 4 are 78, 69, and 63 counts, respectively, suggesting that the source is variable. If Hen 2-90 is the  $\gamma$ -ray source, then it may be a binary in which the primary is a cool giant (as above), but the companion is a neutron star or a black hole. In this case, the ionizing UV flux would be provided by the accretion luminosity. We did not find X-ray emission at the position of Hen 2-90 in the *ROSAT* All-Sky Survey (RASS), but since RASS exposure times were relatively short (1.5 ks) and *ROSAT* was only sensitive to soft X-rays (0.1–2.4 keV) which may be absorbed by the edge-on accretion disk, X-ray emission from Hen 2-90 is not ruled out. The  $H\alpha$  profile toward the Hen 2-90 core shows extended non-Gaussian wings that could arise from gas in Keplerian rotation in the accretion disk, although CFPM93 interpret the wings in terms of a fast ( $\sim 1050 \text{ km s}^{-1}$ ) stellar wind. In summary, our most likely hypothesis for explaining Hen 2-90 requires a binary with a cool giant and a compact companion with an accretion disk. We think that Hen 2-90 provides the strongest empirical evidence so far for a common physical mechanism for generating collimated outflows in protostars and evolved stars. Multiwavelength, multi-epoch observations, especially in the infrared and X-ray bands, are critically needed to elucidate the true nature of this unique object.

R. S. acknowledges helpful discussions with N. Soker, K. Borkowski, D. Meier, K. Stapelfeldt, and W. Brandner; the latter brought to our attention the  $\gamma$ -ray source. We thank our anonymous referee for helpful comments. Financial support for this work was provided by NASA through grant GO-08345.01-97A from the Space Telescope Science Institute and a Long Term Space Astrophysics grant (399-30-61-00-00). SEST is operated jointly by ESO and the Swedish National Facility for Radio Astronomy, Onsala Space Observatory at Chalmers University of Technology.

#### REFERENCES

- Acker, A., Ochsenbein, F., Stenholm, B., Tylenda, R., Marcout, J., & Schohn, S. 1992, *Strasbourg-ESO Catalog of Galactic Planetary Nebulae* (Garching: ESO)
- Burrows, C. J., et al. 1996, *ApJ*, 473, 437
- Corradi, R. L. M., Brandi, E., Ferrer, O. E., & Schwarz, H. E. 1999, *A&A*, 343, 841
- Costa, R. D. D., de Freitas Pacheco, J. A., & Maciel, W. J. 1993, *A&A*, 276, 184
- Egan, M. P., et al. 1999, *US Air Force Res. Lab. Tech. Rep. AFRL-VS-TR-1999-1522*
- Garcia-Lario, P., Manchado, A., Riera, A., Mampaso, A., & Pottasch, S. R. 1991, *A&A*, 249, 223
- Harrington, J. P., & Borkowski, K. J. 2000, in *ASP Conf. Ser. 199, Asymmetrical Planetary Nebulae II. From Origins to Microstructures*, ed. J. H. Kastner, N. Soker, & S. Rappaport (San Francisco: ASP), 383
- Hartman, R. C., et al. 1999, *ApJS*, 123, 79
- Henize, K. 1967, *ApJS*, 14, 125
- Hollis, J. M., Lyon, R. G., Dorband, J. E., & Feibelman, W. A. 1997, *ApJ*, 475, 231
- Jura, M. 1986, *ApJ*, 303, 327
- Kafatos, M., Hollis, J. M., Yusef-Zadeh, F., Michalitsianos, A. G., & Elitzur, M. 1989, *ApJ*, 346, 991
- Kaler, J. B., & Jacoby, G. 1991, *ApJ*, 372, 215
- Kimeswenger, S. 1998, *MNRAS*, 294, 312

- Lamers, H. J. G. L. M., Zickgraf, F.-J., de Winter, D., Houziaux, L., & Zorec, J. 1998, *A&A*, 340, 117
- Maciel, W. J., & Dutra, C. M. 1992, *A&A*, 262, 271
- Martí, J., Rodríguez, L. F., & Reipurth, B. 1993, *ApJ*, 416, 208
- Morris, M. 1987, *PASP*, 99, 1115
- Perek, L., & Kohoutek, L. 1967, *Catalogue of Galactic Planetary Nebulae* (Prague: Publ. House Czech. Acad. Sci.)
- Poetzels, R., Mundt, R., & Ray, T. P. 1989, *A&A*, 224, L13
- Pottasch, S. R., Bignell, C., Olling, R., & Zijlstra, A. A. 1988, *A&A*, 205, 248
- Preite-Martinez, A., Acker, A., Koeppen, J., & Stenholm, B. 1991, *A&AS*, 88, 121
- Purton, C. R., Feldman, P. A., Marsh, K. A., Allen, D. A., & Wright, A. E. 1982, *MNRAS*, 198, 321
- Sahai, R., & Trauger, J. T. 1998, *AJ*, 116, 1357
- Sahai, R., Wootten, A., Schwarz, H. E., & Clegg, R. E. S. 1991, *A&A*, 251, 560
- Swings, J. P., & Andrillat, Y. 1979, *A&A*, 74, 85
- Taylor, A. R., & Seaquist, E. R. 1984, *ApJ*, 286, 263
- Volk, K., & Cohen, M. 1990, *AJ*, 100, 485
- Wood, P. R., & Faulkner, D. J. 1986, *ApJ*, 307, 659